Progress in Physics of Applied Materials 1 (2021) 57–62

Semnan University

Progress in Physics of Applied Materials

journal homepage: https://ppam.semnan.ac.ir/

Light propagation and optical filtering properties of one dimensional Pascal plasma photonic multilayers

*D. Haji Taghi Tehrani, M. Solaimani**

Department of Physics, Qom University of Technology, Qom, Iran

ARTICLE INFO

Article History:
Received:11 August 2021
Revised: 4 October 2021
Accepted:19 October 2021

Keywords:
Pascal-type photonic multilayers light transport
transmission coefficient
transfer matrix method

ABSTRACT

We numerically study the propagation of electromagnetic waves in Pascal plasma photonic crystals. For this purpose, the transfer matrix method is used. This method is based on defining multiple matrices for moving waves in interfaces and layers. Other methods such as finite difference time range can also be used, but are more suitable for higher-dimensional photonic crystals. We investigate the effect of dielectric layer refractive index, plasma electron density, total system length, wavelength angle, and the number of photon crystal layers on the transfer coefficient. A pseudo-code to create the Pascal multilayer is also presented. Finally, we describe the properties of the photonic bandgap, including position and width, because the parameters mentioned are different. We showed that as the refractive index n_1 increases, the position of the gaps alternates redshifted and blueshifted (ie, decreasing and increasing the frequency and energy of the photon). Also, with increasing the refractive index n_1, the width of the gaps decreased and increased. As the collision angle θ_0 grew, the transmission edge blueshifted.

1. Introduction

Photonic crystals are usually defined as artificial structures possessing periodic or quasi-periodic refractive indices [1]. The incident light scatters at the interfaces of the photonic crystals. The superposition of scattering waves can produce photonic bandgaps that are analogous to the electronic bandgap structure in a semiconductor system. Since the first discovery of photonic crystals in 1987 [2-3]. they have found wide applications in optical devices, including optical fibers [4], absorbers [5], filters [6], and sensors [7]. In photonic bandgaps, the electromagnetic wave propagation is prohibited due to the Bragg scattering interference concept. So far, the researchers have used different dispersive or dissipative media to build a tunable photonic crystal, including semiconductors [8], metals [9], and plasma [10], superconductors [11]. In 2004, the terminology of plasma photonic crystals was first introduced by Hojo and co-workers [12]. According to them, the plasma photonic crystals is an efficient way of employing the plasma properties in microwave range [13]. Thereafter, they obtained potential utilizations in different devices, including the filter [14], omnidirectional reflector [15], and optical switching [16].

To produce the photonic multilayer, different arrangements of the alternative layers such as constant total length photonic crystals [17] have so far been investigated. However, quasi-periodic structures with layer placed based on a recursion relation have crucial importance because they can exhibit different exciting properties. The most well-known sequences are Fibonacci [18], Cantor [19], Thue-Mores sequence [20], and the respectively. Besides, the optical properties of graphene mono- and multilayers [21], rectangular to semi-sinusoidal layers [22], three-component photonic crystals [23], nonlinear photonic crystals [24], photonic crystals comprising three phases nanocomposite layer [25], Photonic Crystals with a Staggered Structure [26], ternary plasma photonic crystals [27], Plasma Photonic Crystals Having Exponentially Graded Materials [28], disordered photonic crystals [29], double graded hyperbolic, exponential and linear index materials embedded one-dimensional photonic crystals [30], cylindrical magnetized plasma photonic crystals [31], photonic crystals containing graphene-based hyperbolic metamaterials [32], photonic crystals of porous silicon [33], photonic crystals including MoS2 monolayer [34], photonic crystals composed of plasma and mu-negative materials [35], hybrid multifunctional YaBa2Cu3O7 photonic crystals [36], etc.

In the current paper, we have described the optical transmission through one-dimensional Pascal plasma photonic crystals utilizing the transfer matrix method. Up to our knowledge this structure has not been so far

* Corresponding author. Tel.: +98-919-3754809
E-mail address: Solaimani@qut.ac.ir

DOI: 10.22075/PPAM.2021.24218.1013

studied. The transfer matrix method is based on defining some matrices for traveling waves in interfaces and the layers. Other methods such as finite difference time domain can also be used but it is more appropriate for higher-dimensional photonic crystals. However, for one dimensional photonic crystal, the transfer matrix method is more efficient and faster. This paper is organized as follows. In section 2, we have presented the mathematical backbone of the present papers in addition to the algorithm to produce the Pascal photonic crystal refractive index profile. In section 3, we have described the obtained figures. Finally, in the conclusion section we have present some concluding sentences.

2. Formalism

The periodic or quasi-periodic nature of refractive index changes for a typical photonic crystal leads to the photonic bandgaps. Here, we create the photonic crystal with a refractive index profile according to the Pascal triangle arrangement. In figure 1, we have presented the variation of the refractive index n as a function of the position x. each layer is devoted to a material type (e.g. plasma or dielectric). Layers are alternatively composed of plasma with electron density n_e and dielectric material with refractive index n_1. Two configurations of the Pascal plasma photonic crystals are presented in panels (A) and (B).

The entry of each row and column in Pascal's triangle obeys this formula $\binom{n}{k} = \frac{n!}{k!(n-k)!}$. Where n and k indicate n^{th} row and k^{th} column of Pascal's triangle respectively. That is, to produce all columns of one row, all possible combinations of n should be generated. Let us denote all entries of one row by A_n. Here, we have used A_n to construct two potentials v_1 and v_2. The width of each layer v_1 is directly proportional to each entry of A_n, while layers' width v_2 is inversely proportional to entries of A_n. The amplitude of v_1 and v_2 is set to zero, except for their odd layers where the amplitude is one.

Table 1 shows Algorithm to produce the Pascal photonic crystal refractive index profile. A one-dimensional Pascal plasma photonic crystal is assumed. The plasma layer is created from a solid-state plasma. We utilize the plasma and dielectric refractive indices as n_1 and n_p, respectively. Besides, by assuming a non-magnetized cold plasma, we can use $n_p = \left(1 - w_p^2 / w^2\right)^{1/2}$. Where, $w_p = \left(n_e e^2 / m e_0\right)^{1/2}$ m, n_e, and e is the plasma frequency, the electron mass, electronic plasma density, and electron charge, respectively [37].

Table 1
Algorithm to produce the Pascal photonic crystal refractive index profile

Algorithm v_1 and v_2

Input: n
Output: Matrix v_1 and v_2

1. For k = 0 To n Step 1
2. A_n(k) = n choose k
3. For k = 0 To n Step 1
4. If k corresponds to odd layer
5. Add A_n(k) ones to v_1
6. Add $SUM(A_n(\text{k}))/A_n(\text{k})$ ones to v_2
7. Else
8. Add A_n(k) zeros to v_1
9. Add $SUM(A_n(\text{k}))/A_n(\text{k})$ zeros to v_2

For the TE (TM) electromagnetic wave, the electric field (magnetic field) is assumed to be perpendicular to the planes of the photonic crystals. The electric and magnetic fields at two positions in the adjacent layers are related by [38],

$$M\left[\Delta z\right] = \begin{bmatrix} cos(k_z^j \Delta z) & \dfrac{-i\, sin(k_z^j \Delta z)}{p_i} \\ -i\, p_i sin(k_z^j \Delta z) & cos(k_z^j \Delta z) \end{bmatrix} \tag{1}$$

Where $k_z^j = (\omega / c)\, n_j cos(\theta_j)$ is the z-component of the wave vector in the layer. Also, $p_j = \sqrt{\varepsilon_j / \mu_j} cos(\theta_j)$, where $\cos\theta_j = \sqrt{1-(n_0^2 sin^2\theta_0 / n_j^2)}$. Moreover, c and θ_j are the speed of light in vacuum and the beam angle in layer j. n_0 is also the refractive index of the free space and $n_j = \sqrt{\varepsilon_j \mu_j}$ denotes the k^{th} layer refractive index [39], where, ε_i and μ_i are the permittivity and the permeability of the k^{th} layer materials, respectively. Then, the total transfer matrix due to the N-layers reads,

$$M^{Tot} = \prod_{j=1}^{N} M_j = \begin{bmatrix} M_{11} & M_{12} \\ M_{21} & M_{22} \end{bmatrix} \tag{2}$$

The dimensionless transmission coefficient can now be written as,

$$t = \frac{2p_0}{\left(M_{11} + M_{12} p_s\right) p_0 + (M_{21} + M_{22} p_s)} \tag{3}$$

where $p_0 = n_0 cos(\theta_0)$ and $p_s = n_s cos(\theta_s)$, where n_0, n_s are the environment refractive indices before the first layer and after the last layer, respectively. Also, θ_0 and θ_s are the incident angle and the angle at which the light wave departs from the photonic crystal, respectively. The TM waves are also described by using $p_j = \sqrt{\mu_j / \varepsilon_j} cos(\theta_j)$, $p_0 = cos(\theta_0)/n_0$ and $p_s = cos(\theta_s)/n_s$ [40]. The associated transmittance T of the multilayer is obtained using

$$T = \frac{p_s}{p_0} |t|^2 \tag{4}$$

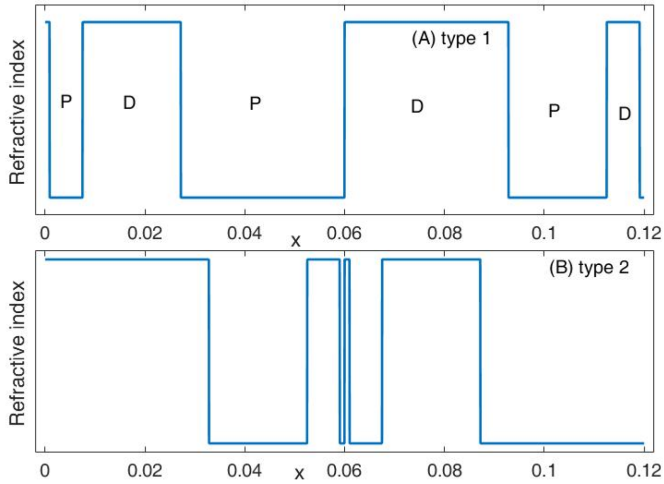

Fig. 1. Variation of the refractive index n as a function of the position x. each layer is devoted to a material kind. Layers alternatively composed from plasma with electron density n_e and dielectric material with refractive index n_1. P and D indicate the plasma and dielectric layers, respectively. Two configurations of the Pascal plasma photonic crystals are presented in panels (A) and (B)

3. Results and Discussion

In the present study, we investigated the optical transmission properties of an ω-frequency electromagnetic wave through some of the plasma Pascal photonic crystals. In each figure, the effect of seven values of a usual parameter is considered, unless otherwise stated. From Fig. 2 onwards, note that all transmission coefficients are between zero and one. It is only for presentation and comparison that the various modes are stacked

Figure 2 presents the variation of the transmission coefficient T as a function of the incident electromagnetic wave frequency ω for some type 1 plasma photonic crystals. The effect of seven different values on the number of layers (NOL) is compared. We also assumed θ0=0, ne=2E19, n1=3, L=60mm. Fig.3 is also the same as Fig. 2, but for some type 2 plasma photonic crystals. When a traveling electromagnetic wave enters a multilayer system, some part of it reflects and some portion transmits. The transmitted wave from layer I can reflect from layer i+1. Then these waves can interfere. According to this interference concept, we can describe the electromagnetic wave transmission through a thick multilayer. Because the constructive and deconstructive interference can lead to passband and bandgaps in the diagram of the transmission coefficient as a function of the incident wave frequency ω. When the transmissions coefficient reaches 1, cent percent transmission occurs. However, if the transmissions coefficient vanishes, then the propagation of the wave with that e=frequency becomes forbidden. As Figs. 2 and 3 show, increasing the number of layers (NOL) leads to changing the position of the bandgap and passbands because changing the arrangement and thickness of the layers leads to different interference situations. In both Figs. 2 and 3, the initial transmission edge for approximately all systems is about 40 GHz. Although a slight deviation from this frequency is visible. In the following, we restrict ourselves to the interval [40 to 60] GHz for the type 1 structure.

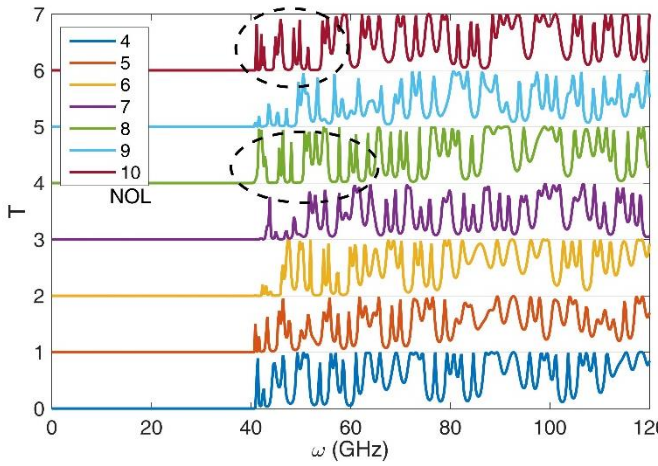

Fig. 2. Variation of the transmission coefficient T as a function of the incident electromagnetic wave frequency ω for some type 1 plasma photonic crystals. Effect of seven different values of the number of layers (NOL) are compared. We also assumed θ_0=0, n_e=2E19, n_1=3, L=60mm

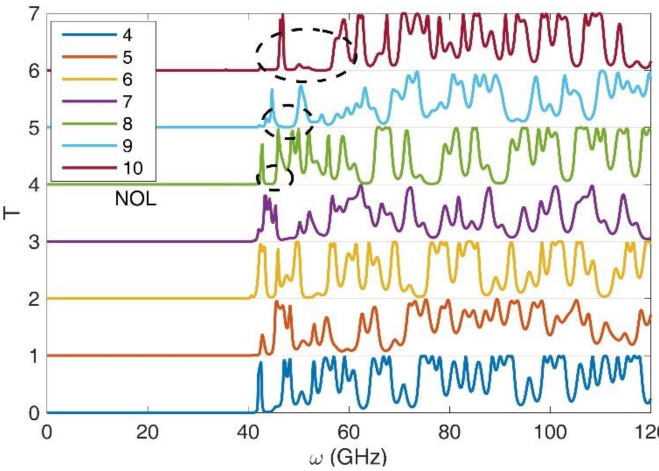

Fig. 3. The same as figure 2, but for some type 2 plasma photonic crystals

In Fig. 4, we have depicted the variation of the transmission coefficient T as a function of the incident electromagnetic wave frequency ω for some type 1 plasma photonic crystals. The effect of seven different values of the system total lengths L are compared. We also assumed θ_0=0, n_e=2E19, n_1=3, L=60mm, and NOL=10. As one can see, by changing L, different gap widths are created. Thus, L can be a good tuning tool. In the figure, we have illustrated the gap position shifts by some arrows when L changes. As these arrows show, by increasing L, some gaps' position blueshift (i.e., move toward higher frequencies), while the other redshift. Therefore, using L increment we can regulate the gap position too. Another fact is that, by increasing L, roughly speaking, the number of peaks in the diagram of the transmission versus wave frequency increases.

Figure 5 shows the variation of the transmission coefficient T as a function of the incident electromagnetic wave frequency ω for some type 1 plasma photonic crystals. The effect of seven different values of the dielectric refractive index n_1 is compared. We also assumed $\theta_0=0$, n_e=2E19, L=60mm, and NOL=10. In this figure, as the refractive index n_1 increases, the gaps' position alternatively redshift and blueshift. We have illustrated this fact using the dashed and dotted arrows. As one may see, the arrows are alternatively placed. Also, there are some flat transmission passbands in the range of 50 to 60 GHz for some systems. Finally, as the refractive index n_1 increases, the widths of the gaps alternatively decrease and increase.

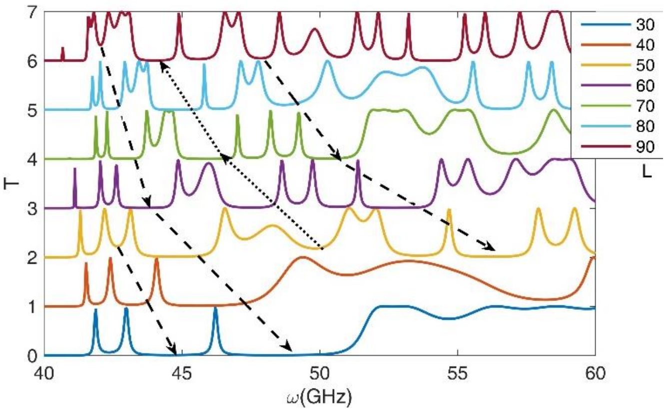

Fig. 4. Variation of the transmission coefficient T as a function of the incident electromagnetic wave frequency ω for some type 1 plasma photonic crystals. Effect of seven different values of the system total lengths L is compared. We also assumed $\theta_0=0$, n_e=2E19, n_1=3, L=60mm, and NOL=10

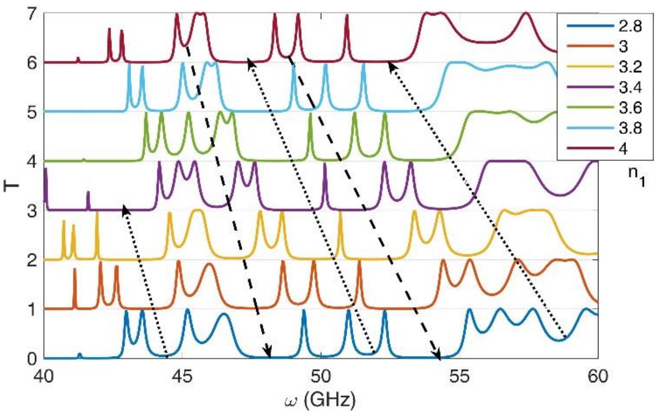

Fig. 5. Variation of the transmission coefficient T as a function of the incident electromagnetic wave frequency ω for some type 1 plasma photonic crystals. Effect of seven different values of the dielectric refractive index n_1 is compared. We also assumed $\theta_0=0$, n_e=2E19, L=60mm, and NOL=10

In Fig. 6, we have presented the variation of the transmission coefficient T as a function of the incident electromagnetic wave frequency ω for some type 1 plasma photonic crystals. Effect of seven different values of the plasma layer electron densities n_e is compared. We also assumed $\theta_0=0$, n_1=3, L=60mm, and NOL=10. It is seen that, for small values of the plasma electron density n_e, the two marked gapes blueshift. However, for high values of ne, the left gap blueshift, while the other redshift. Another fact is that, by increasing n_e, the gap widths increase and become pore flat (i.e., more perfect gaps). Finally, figure 7 presents the variation of the transmission coefficient T as a function of the incident electromagnetic wave frequency ω for some type 1 plasma photonic crystals. The effect of three different values of the angle θ_0 is compared. We also assumed n_e=2E19, n_1=3, L=60mm, and NOL=10. As this figure shows, when θ_0 increases, the transmission edge blueshift.

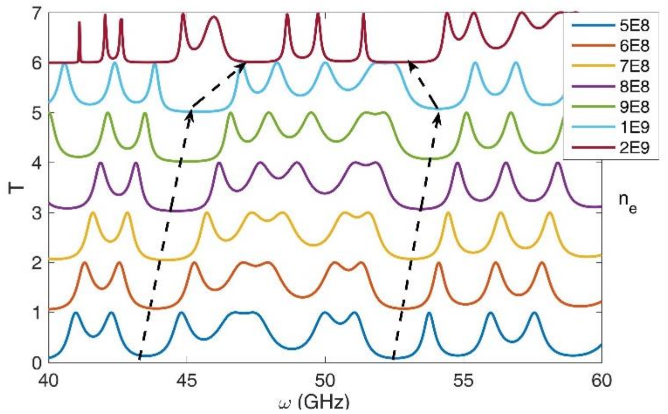

Fig. 6. Variation of the transmission coefficient T as a function of the incident electromagnetic wave frequency ω for some type 1 plasma photonic crystals. Effect of seven different values of the plasma layer electron densities n_e (cm^{-3}) are compared. We also assumed $\theta_0=0$, n_1=3, L=60mm, and NOL=10

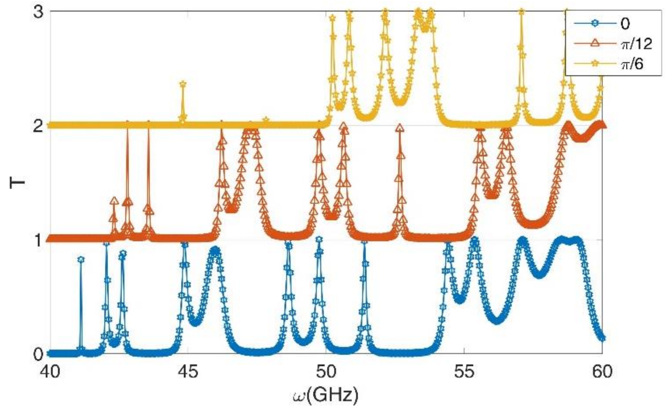

Fig. 7. Variation of the transmission coefficient T as a function of the incident electromagnetic wave frequency ω for some type 1 plasma photonic crystals. Effect of three different values of the angle θ_0 are compared. We also assumed n_e=2E19, n_1=3, L=60mm, and NOL=10

4. Conclusions

In this work, we investigated the transfer properties of single-dimensional Pascal plasma photon crystals. It is shown that the initial transmission edge for our proposed structures was about 40 GHz. As L increases, some gaps' position is blueshifted, while others redshifted and it seemed they do not follow an order. But, as the refractive index n_1 increased, the gaps' position alternatively redshifted and blueshifted. Also, as the refractive index n_1 increased, the widths of the gaps alternatively decreased and increased. When θ_0 increased, the transmission edge blueshifted.

References

[1] M. Solaimani, M. Ghalandari, and M. Nejati, "Optical filters based on fixed length Thue–Morse plasma-dielectric photonic band multilayers: Comparing two, three, and four materials systems," AIP Advances, 11 (2021) 025309.

[2] E. Yablonovitch, "Inhibited spontaneous emission in solid-state physics and electronics," Phys. Rev. Lett. 5 (1987) 2059.

[3] S. John, "Strong localization of photons in certain disordered dielectric superlattices," Phys. Rev. Lett. 58 (1987) 2486.

[4] F. Benabid, J. C. Knight, G. Antonopoulos and P. J. Russell St, "Stimulated Raman scattering in hydrogen-filled hollow-core photonic crystal fiber," Science 298 (2002) 399.

[5] S.P. Li, H.J. Liu, Q.B. Sun and N. Huang, "A tunable terahertz photonic crystal narrow-band filter," IEEE Photonic Tech. Lett. 27 (2015) 752.

[7] X. Zhu, X. D. Yang and X. Wang, Prog. Electromagn. Res. 67 (2017) 103.

[8] M. Kamp, T. Happ, S. Mahnkopf, G. Duan, S. Anand, A. Forchel, "Semiconductor photonic crystals for optoelectronics," Physica E, 21 (2004) 802.

[9] N.N. Lepeshkin, A. Schweinsberg, G. Piredda, R.S. Bennink, R.W. Boyd, "Enhanced nonlinear optical response of one-dimensional metal-dielectric photonic crystals," Phys. Rev. Lett. 93 (2004) 123902.

[10] H.F. Zhang, S.B. Liu, X.K. Kong, L. Zhou, C.Z. Li, and B. R. Bian, "Enlarged omnidirectional photonic bandgap in heterostructure of plasma and dielectric photonic crystals," Optik, 124 (2013) 751.

[11] H. F. Zhang, S. B. Liu, Y. Y. Zhu, X. K. Kong, B. R Bian, X. Zhao, "Properties of omnidirectional photonic bandgaps in Fibonacci quasi-periodic one-dimensional superconductor photonic crystals," Prog Electromagn. Res. B, 40 (2012) 415–431.

[12] H. Hojo, A. Mase, "Dispersion relation of electromagnetic waves in one dimensional plasma photonic," J. Plasma Fusion Res. 80 (2004) 89–90.

[13] H. F. Zhang, S. B. Liu, and X. K. Kong, "Defect mode properties of two-dimensional unmagnetized plasma photonic crystals with line-defect under transverse magnetic mode," Acta Phys. Sin. 60 (2011).

[14] C. Li, S. Liu, X. Kong, H. Zhang, B. Bian, and X. Zhang, "A novel comb-like plasma photonic crystal filter in the presence of evanescent wave," IEEE Trans. Plasma Sci. 39 (2011) 1969–1973.

[15] H.F. Zhang, S.B. Liu, X.K. Kong, L. Zou, C.Z. Li, and W.S. Qing, "Enhancement of omnidirectional photonic bandgaps in one-dimensional dielectric plasma photonic crystals with a matching layer," Phys. Plasmas 19 (2012) 022103–022107.

[16] H.F. Zhang and S.B. Liu, "Magneto-optical Faraday effects in dispersive properties and unusual surface plasmon modes in the three-dimensional magnetized plasma photonic crystals," IEEE Photonics, 6 (2014) 5300112.

[17] M. Solaimani, M. Ghalandari, A. Aghajamali, "Bandgap engineering in constant total length nonmagnetized plasma-dielectric multilayers," Optik, 207 (2020) 164476.

[18] H.F. Zhang, S.B. Liu, X.K. Kong, B.R. Bian, Y. Dai, "Omnidirectional photonic bandgap enlarged by one-dimensional ternary unmagnetized plasma photonic crystals based on a new Fibonacci quasiperiodic structure," Phys. Plasmas, 19 (2012) 112102.

[19] A.V. Lavrinenko, S.V. Zhukovsky, K.S. Sandomirski, S. V. Gaponenko, "Propagation of classical waves in nonperiodic media: Scaling properties of an optical Cantor filter," Phys. Rev. E. 65 (1990) 036621.

[20] X.L. Quan, X.B. Yang, "CLASSICAL AREAS OF PHENOMENOLOGY: Band rules for the frequency spectra of three kinds of aperiodic photonic crystals with negative refractive index materials," Chin. Phys. B, 18 (2009) 5313-5325.

[21] L.A. Falkovsky, S.S. "Pershoguba, Optical far-infrared properties of a graphene monolayer and multilayer," Phys. Rev. B 76 (2007) 153410.

[22] M. Solaimani, "Optical transport properties of one dimensional plasma photonic crystals: Crossover from rectangular to semi-sinusoidal layers," Results in Physics 16 (2020) 102843.

[23] Vladimir A. Tolmachev, Anna V. Baldycheva, Sergey A. Dyakov, Kevin Berwick, and Tatiana S. Perova, "Optical Contrast Tuning in Three-Component One-Dimensional Photonic Crystals," J. Lightwave Technol. 28 (2010) 1521-1529.

[24] L.M. Zhao, B.Y. Gu, Y.S. Zhou, "A way for enhancing second harmonic generation in one-dimensional nonlinear photonic crystals," Optics Communications, 281 (2008) 2954–2958.

[25] A. GMohamed, H.A. ElSayed, A. Mehaney, A.H. Aly and W. Sabra, "The transmissivity of one-dimensional photonic crystals comprising three phases nanocomposite layer for optical switching purposes," Phys. Scr. 96 (2021) 115504.

[26] H.F. Zhang, S.B. Liu, X.K. Kong, B.R. Bian, B. Ma, "Enhancement of Omnidirectional Photonic Bandgaps in One-Dimensional Superconductor–Dielectric Photonic Crystals with a Staggered Structure," J. Supercond. Nov. Magn. 26 (2013) 77-85.

[27] X.K. Kong, S.b. Liu, H.F. Zhang, C.Z. Li, B.R. Bian, "Omnidirectional photonic bandgap of one-dimensional ternary plasma photonic crystals," J. Opt. 13 (2011) 035101.

[28] S. Prasad, V. Singh and A.K. Singh, "Study on the Reflection Spectra of One Dimensional Plasma Photonic Crystals Having Exponentially Graded Materials,"Plasma Sci. Technol. 15 (2013) 443.

[29] J.H. Wu, M. Artoni, and G.C. La Rocca, "Perfect absorption and no reflection in disordered photonic crystals," Phys. Rev. A 95 (2017) 053862.

[30] B.K Singh, A. Bijalwan, P.C. Pandey, V. Rastogi, "Photonic bandgaps engineering in double graded hyperbolic,exponential and linear index materials embedded one-dimensional photonic crystals," Eng. Res. Express, 1 (2019) 025004.

[31] Q.Y. Wang, S. Liu, D. Gui and H.F. Zhang, "Nonreciprocal absorption characteristics of one-dimensional

cylindrical magnetized plasma photonic crystals," Phys. Scr. 96 (2021) 065501.
[32] A. Madani, S. Roshan Entezar, "Optical properties of one-dimensional photonic crystals containinggraphene-based hyperbolic metamaterials," Photonics and Nanostructures – Fundamentals and Applications, 25 (2017) 58–64.
[33] I.A. Lujan-Cabrera, C.F. Ramirez-Gutierrez, J.D. Castaño-Yepes, M.E. Rodriguez-Garcia, "Effects of the interface roughness in the optical response of one-dimensional photonic crystals of porous silicon," Physica B: Condensed Matter, 560 (2019) 133–139.
[34] N. Ansari, E. Mohebbi, "Increasing optical absorption in one-dimensional photonic crystals including MoS2 monolayer for photovoltaics applications," Optical Materials, 62 (2016) 152-158.
[35] Y. Liu, L. Yi, X.G. Hu, Y.-F. Duan, and Z.-Z. Yang, "Phase retarder based on one-dimensional photonic crystals composed of plasma and mu-negative materials," Physics of Plasmas, 22 (2015) 012101.
[36] A.H. Aly, S.E.S. Abdel Ghany, B.M. Kamal, D. Vign, "Theoretical studies of hybrid multifunctional YaBa2Cu3O7 photonic crystals within visible and infra-red regions," Ceramics International, 46 (2020) 365–369.
[37] Z. Naderi Dehnavi, H. Ranjbar Askari, M. Malekshahi, and D. Dorranian, "Investigation of tunable omnidirectional bandgap in 1D magnetized full plasma photonic crystals," Physics of Plasmas, 24 (2017) 093517.
[38] A. Aghajamali, M. Barati, "Effects of normal and oblique incidence on zero-n gap in periodic lossy multilayer containing double-negative materials," Physica B, 407 (2012) 1287-1291.
[39] L. Zhang, Y. Zhang, L. He, Z. Wang, H. Li, H. Chen, "Zero- n gaps of photonic crystals consisting of positive and negative index materials in microstrip transmission lines," J. Phys. D. Appl. Phys. 40, (2007) 2579-2583.
[40] P. Yeh, "Optical waves in layered media," Wiley Series in Pure and Applied Optics, (1988).